Acta Astronautica 79 (2012) 131–139

Contents lists available at SciVerse ScienceDirect

Acta Astronautica

journal homepage: www.elsevier.com/locate/actaastro

A feedback linearization control for the nonlinear 5-DOF flywheel suspended by the permanent magnet biased hybrid magnetic bearings

Wen Tong*, Fang Jiancheng

School of Instrumentation Science and Opto-Electronics Engineering, Science and Technology on Inertial Laboratory, Beijing University of Aeronautics and Astronautics, Beijing, China

ARTICLE INFO

Article history:
Received 16 August 2011
Received in revised form
29 March 2012
Accepted 10 April 2012
Available online 16 May 2012

Keywords:
Magnetic bearing
Nonlinear control
Exact linearization
Luenberger observer
State feedback

ABSTRACT

The dynamic model of the magnetic suspension flywheel (MSFW) whose rotor is suspended by the permanent magnet (PM) biased hybrid magnetic bearing is nonlinear, complicated and coupled because of the superposition and couple of the electromagnetic flux and PM flux. It is a challenge for the closed-loop controller design of the MSFW. In this paper, the MIMO nonlinear dynamic model of such MSFW has been obtained using the equivalent magnetic flux circuit calculation and integrating the rotor dynamics. A nonlinear Luenberger observer has been designed to estimate the state variables of the system, and then the dynamic model has been exact linearized to linear and decoupled one using the state feedback. At last, a linear controller has been designed based on the obtained exact linearization model. The better abilities of decoupling and disturbance depression of the proposed controller compared to the controllers designed based on the Taylor linearization model are verified by simulations and experiments.

1. Introduction

The non-contact character of the active magnetic bearing (AMB) brings up many advantages over the traditional ball bearings, such as high rotation speed, nearly zero friction, long life-span, absence of auxiliary lubrication system and so on [1–3]. The magnetic suspension flywheel which utilizes the AMBs to support the rotor non-contactly is regarded as the promising actuator for the spacecraft attitude control [4–6]. There are two major kinds of the AMBs used in the MSFW system. The first one is the electromagnetic bearing (EMB), whose suspending forces for rotor are generated by the coil currents totally. The other one is the PM biased HMB, whose permanent magnets provide the biased flux, and currents generate the regulating forces to realize the stable suspension of the rotor. As only electronic magnetic flux in the EMB, the dynamic model of the rotor-EMB of the MSFW is simpler relatively. But the power consumption is greater because the biased flux is generated by the biased current. The power consumption is reduced greatly in the application of the PM biased HMB, because the biased flux is proved by the permanent magnet without any external power consumption.

An effective controller is needed for the MSFW because of the instability of the open-loop AMB caused by the negative displacement stiffness of the magnetic force [7,8]. Many control strategies have been applied to stabilize the EMB successfully, such as sliding model control [9,10], adaptive robust nonlinear control [11,12], output feedback stepping control [13] and so on. The dynamic model of the PM biased HMB is nonlinear and complicated, and its nonlinearity is caused by the superposition of PM flux and EM flux and the

* Corresponding author. Tel.: +86 10 82317396; fax: +86 10 82316813.
E-mail address: wentong@aspe.buaa.edu.cn (W. Tong).

0094-5765/$ - see front matter © 2012 Elsevier Ltd. All rights reserved.
http://dx.doi.org/10.1016/j.actaastro.2012.04.017

magnetic flux coupling in different directions. Generally, the permanent magnet in HMB is regarded as an equivalent biased current in the EMB, so an equivalent EMB-like model describing the HMB system will be obtained. Based on the equivalent model, using the Taylor series expansion in the neighborhood of the operating point, an approximate linear model of the nonlinear HMB system is obtained for the controller design. This method has an obvious advantage that the control model is very simple and the controller can be realized simply. For the application of the HMB with high restriction on power loss and accuracy, such as MSFW, the controller design must be based on the nonlinear model of system. The biased magnetic fluxes in different HMBs are provided by one permanent magnetic ring, the eccentricity between the stator and the rotor could causes the magnetic flux coupling between the different HMBs. So the dynamics model is coupling in different DOFs. Besides the nonlinear and coupling of the dynamic model, the rotor suffers the disturbances caused by the residual unbalance masses when the rotor is spinning rapidly.

To settle the nonlinear, coupling and disturbance problems mentioned above, a nonlinear controller of the HMB for the MSFW has been developed in this paper. This paper is organized as follows. In Section 2, the dynamic model of the rotor-HMBs of the MSFW has been obtained using magnetic flux law and rotor dynamics. In Section 3, a standard MIMO Luenberger nonlinear observer has been developed based on the obtained dynamic model. Using the state estimates, an exact linearization method has been introduced to the control of the HMB in Section 4, and then a simple linear controller has been designed to stabilize the unstable rotor-HMB of the MSFW system. The simulation and experiment results have been shown in Section 5 to verifier the validity of the exact linearization control strategy for the MSFW system.

2. Model development

As shown in Fig. 1, the 5-DOF MSFW consists of rotor, stator, HMBs, displacement sensors, driven motor, basement, seal cover and backup bearings.

For the convenience of model development, there are three coordinate frames introduced in the system, as shown in Fig. 2. *OXYZ* is the stator-fixed frame, *oxyz* is the rotor-fixed frame and *oabc* is the intermediate frame.

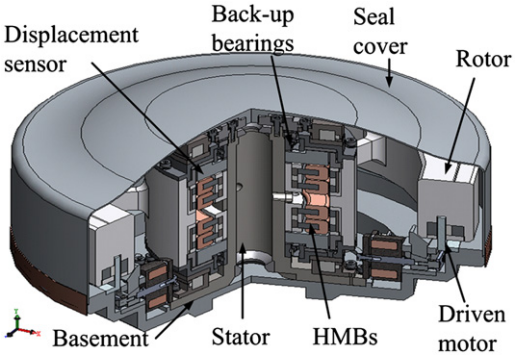

Fig. 1. The sketch of the MSFW utilizing the PM biased HMBs.

The six generalized degrees of freedom (DOFs) of the rotor are $[x, y, z, \alpha, \beta, \Omega]$ and defined by the displacements and Euler-angles between the three frames. The rotation Ω along *oz* direction is controlled by the driven motor and independent of the HMBs. The translation *z* is controlled by the axial HMB and can be regarded as decoupled with other four coupled axial DOFs $[x, y, \alpha, \beta]$. The four axial DOFs of the rotor could be calculated from the four signals picked up by the displacement sensors $[x_{ma}\ y_{ma}\ x_{mb}\ y_{mb}]$ using Eq. (1)

$$\begin{cases} x = x_{ma} + x_{mb} \\ \beta = (x_{ma} - x_{mb})/L \\ y = y_{ma} + y_{mb} \\ \alpha = (y_{ma} - y_{mb})/L \end{cases} \tag{1}$$

L is the distance between the two displacement sensors located at the two ends the stator of the MSFW, as shown in Fig. 3.

So the main task of this paper is to obtain the nonlinear dynamic model of the rotor suspended by the HMBs and then design a controller based on the obtained nonlinear dynamic model.

2.1. Magnetic force

The MSFW includes four sets of radial HMBs. In *OXYZ* frame, four sets of HMBs locate at the *X* and *Y* direction in *A* and *B* sides of stator, respectively. As shown in Fig. 4, it

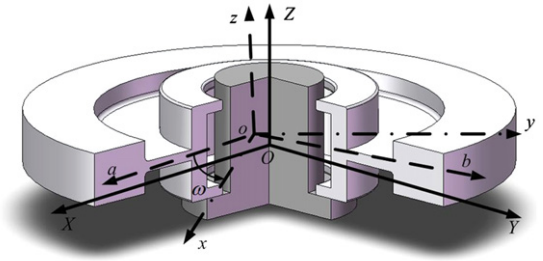

Fig. 2. The frame systems used in the MSFW model development.

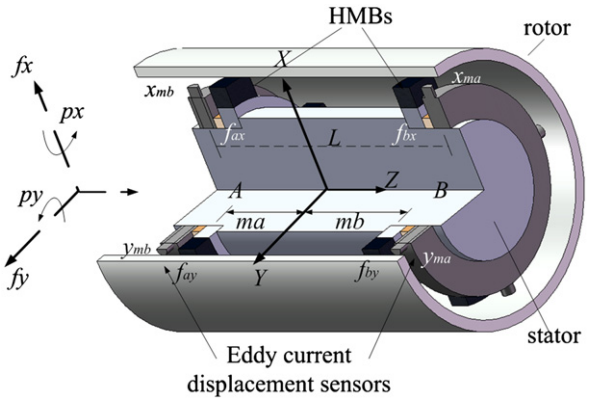

Fig. 3. The details about the forces, torques and displacements of the rotor.

is the sketch of the two set of HMBs located at *A* side of the stator in *X* and *Y* directions. Each one set of HMB is composed of two series connected coils to generate the restoring force together. One magnet ring is embedded in the stator to generate the biased magnetic flux for both of the two HMBs at the *A* side.

The flux paths and equivalent flux circuits of the HMBs are detailed described in Fig. 5.

The magnetic forces are generated by the PM flux and EM flux. When the rotor is out of its equilibrium position with displacement of (x_{ma}, y_{ma}) at *A* side, the air-gap length become to $g-x_{ma}$, $g+x_{ma}$, $g-y_{ma}$, $g+y_{ma}$, as shown in Fig. 5(b). Take the HMB in *X* direction for example. It is assumed that the control current i_{ax} are sent to the opposite connected coils in $X+$ and $X-$. Control currents flowing through the two coils in $X+$ and $X-$ are i_{ax} and $-i_{ax}$, respectively. f_{ax} is the resultant restoring force acting on the rotor, which is the difference between the two magnetic force f_{ax+} and f_{ax-} in $X+$ and $X-$ directions.

$$f_{ax} = f_{ax+} - f_{ax-} = [(\phi_{pax+} + \phi_{iax+} + \phi_{iax-ax+})^2 - (\phi_{pax-} - \phi_{iax-} - \phi_{iax+ax-})^2]/(2\mu_0 A) \quad (2)$$

where ϕ_{pax+}, ϕ_{pax-} are PM flux in air-gap of $X+$ and $X-$, ϕ_{iax+}, $\phi_{iax+ax-}$ are EM flux in $X+$ and $X-$ generated by the control current i_{ax}. $\phi_{iax-ax+}$, ϕ_{iax-} are EM magnetic flux in $X+$ and $X-$ generated by the control current $-i_{ax}$. μ_0 is the permeability of the vacuum and *A* is the area of one pole. The other three magnetic forces f_{ay}, f_{bx} and f_{by} would be obtained using the same methods described above. As following, it is the linear transformation between the generalized forces and the magnetic forces.

$$\begin{bmatrix} f_x \\ p_y \\ f_y \\ p_x \end{bmatrix} = \begin{bmatrix} f_{ax} + f_{bx} \\ ma \cdot f_{ax} - mb \cdot f_{bx} \\ f_{ay} + f_{by} \\ -ma \cdot f_{ay} + mb \cdot f_{by} \end{bmatrix} \quad (3)$$

ma and *mb* are the distances from the HMBs to the origin of the *OXYZ*.

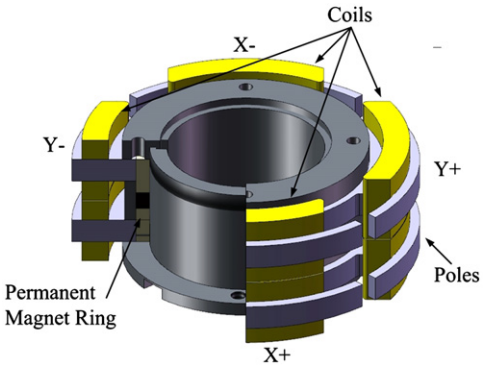

Fig. 4. The stator of the PM biased HMB used in the MSFW.

2.2. Rotor dynamics

As the spin rate of the rotor is lower than 6000 rpm (100 Hz) and lower than the first natural frequency of the

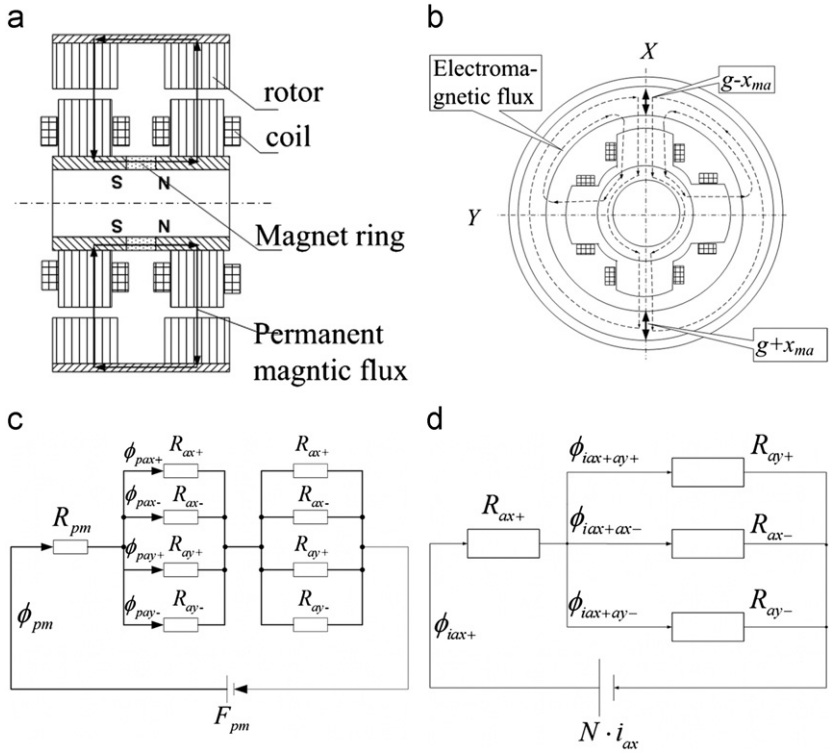

Fig. 5. The equivalent flux circuits of the radial HMBs. (a) The PM flux path generated by the magnet ring, (b) the EM flux path generated by current i_{ax}, (c) the equivalent PM flux circuit of the HMBs and and (d) the equivalent EM flux circuit of the HMBs.

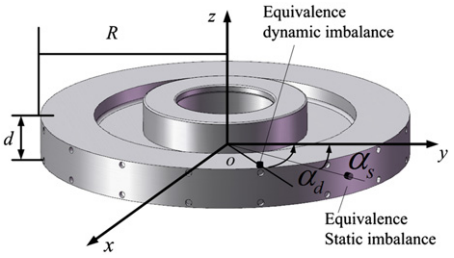

Fig. 6. The rotor with static and dynamic imbalances.

rotor which is above 1.3 kHz, so the rotor is regarded as rigid in its operation spin rate. The rotor of the MSFW is modeled as a balanced wheel. The most significant disturbance sources, static and dynamic imbalances, are added to the rotor to complete the model. They are modeled with lumped masses that are positioned strategically on the wheel. The details of the rotor are described in Fig. 6, the masses and locations of the static and dynamic imbalances are (m_s α_s) and (m_d α_d), respectively in the *oxyz* frame. The state variables are chosen as $x=\left[x\dot{x}\beta\dot{\beta}y\dot{y}\alpha\dot{\alpha}\right]$. The generalized magnetic forces acting on the system are [f_x p_y f_y p_x], so the system dynamic model can be obtained with the generalized forces and rotor dynamic equations. The universal dynamic model of the rapidly spinning rotor is [14],

$$\begin{cases} m\ddot{x}=f_x+\Delta f_x \\ m\ddot{y}=f_y+\Delta f_y \\ J_y\ddot{\beta}-J_z\omega\dot{\alpha}=p_y+\Delta p_y \\ J_x\ddot{\alpha}+J_z\omega\dot{\beta}=p_x+\Delta p_x \end{cases} \tag{4}$$

Δf_x, Δf_y, Δp_x, and Δp_y are the disturbances caused by the residual static and dynamic imbalances.

2.3. Dynamic model of the nonlinear system

As described in Eq. (5), the MSFW is a 4-input, 4-output, 8-order affine nonlinear system.

$$\begin{cases} \dot{x}=f(x)+\sum_{i=1}^{4} g_i(x)u_i+\Delta(t) \\ y=h(x) \end{cases} \tag{5}$$

The dynamics model is consisted of three parts. The first is state equation $f(x)$ which is regarded as the uncontrollable permanent magnetic force and the couple caused by the gyroscopic effect of the rotor. The second is the controllable magnetic force$\sum_{i=1}^{4} g_i(x)u_i$, which is the input part of the system. The inputs of the system are selected as $u=[i_{ax}\ i_{bx}\ i_{ay}\ i_{by}]$. The last one is the disturbances caused by the residual static and dynamic imbalances. The displacements of the rotor in the *OXYZ* [x_{ma} x_{mb} y_{ma} y_{mb}] are defined as the outputs of the system. $h(x)$ is the output function. The details of the dynamic model are described in Eq. (6–13). The state equations of the model are,

$$\begin{aligned} f_1(x)&=x_2 \\ f_2(x)&=\frac{k_1}{m}\left[{p_1}^2\cdot(x_1+ma\cdot x_3)+{p_3}^2\cdot(x_1-mb\cdot x_3)\right] \\ f_3(x)&=x_4 \\ f_4(x)&=\frac{k_1}{J_y}\left[ma\cdot{p_1}^2\cdot(x_1+ma\cdot x_3)-mb\cdot{p_3}^2\cdot(x_1-mb\cdot x_3)\right] \\ &\quad+\cdots\left\{\overline{a}\sin(2\Omega t)\Omega\cdot x_6+\left[\overline{b}+\overline{c}\sin^2(\Omega t)\right]\Omega\cdot x_8\right\} \\ f_5(x)&=x_6 \\ f_6(x)&=\frac{k_1}{m}\left[{p_2}^2\cdot(x_5-ma\cdot x_7)+{p_4}^2\cdot(x_5+mb\cdot x_7)\right] \\ f_7(x)&=x_8 \\ f_8(x)&=\frac{k_1}{J_x}\left[-ma\cdot{p_2}^2\cdot(x_5-ma\cdot x_7)+mb\cdot{p_4}^2\cdot(x_5+mb\cdot x_7)\right] \\ &\quad+\cdots\left\{\left[\overline{d}+\overline{e}\cos^2(\Omega t)\right]\Omega\cdot x_6+\overline{f}\sin(2\Omega t)\Omega\cdot x_8\right\} \end{aligned} \tag{6}$$

where m is the mass of the rotor, J_x and J_y are the moments of inertial of the rotor in x and y directions. $\overline{a}\sim\overline{f}$ are the calculated coefficients.

$$\begin{aligned} &\left\{\overline{a}=-J_d/(J_y+2m_dh^2)\right. \\ &\overline{b}=J_z/(J_y+2m_dh^2) \\ &\overline{c}=2J_d/(J_y+2m_dh^2) \\ &\overline{d}=-J_z/(J_x+2m_dh^2) \\ &\overline{e}=-2J_d/(J_x+2m_dh^2) \\ &\overline{f}=J_d/(J_x+2m_dh^2) \end{aligned} \tag{7}$$

k_1 is the calculated nominal displacement stiffness, and k_2 is the calculated nominal current stiffness.

$$k_1=-(F_{pm}G_{pm})^2/(\mu_0Ag), k_2=4Nk_eGF_{pm}(\mu_0A) \tag{8}$$

F_{pm} is the magnetic potential of the permanent magnet, and G_{pm} is the magnetic conductance of the magnet. k_e is the leakage coefficient of the PM flux circuit.

$$\mathrm{F_{pm}}=\mu_0\mu_rA_{pm}/h_{pm}, \mathrm{G_{pm}}=H_ch_{pm}/k_m \tag{9}$$

μ_r, A_{pm}, h_{pm} and H_c are the relative permeability, cross section, height and coercive force of the permanent magnet, respectively. The four nominal functions commonly used in f_1–f_8 and the input functions g_1–g_4 are defined as follows,

$$\begin{aligned} p_1&=\frac{g^2-y_{ma}^2}{2g^2-x_{ma}^2-y_{ma}^2}, p_2=\frac{g^2-x_{ma}^2}{2g^2-x_{ma}^2-y_{ma}^2} \\ p_3&=\frac{g^2-y_{mb}^2}{2g^2-x_{mb}^2-y_{mb}^2}, p_4=\frac{g^2-x_{mb}^2}{2g^2-x_{mb}^2-y_{mb}^2} \end{aligned} \tag{10}$$

The input functions of the nonlinear system are described in detail as follows.

$$g_1(x)=k_2\begin{bmatrix}0\\0\\0\\0\\\frac{p_1}{m}\\\frac{ma\cdot p_1}{J_x}\\0\\0\end{bmatrix}\quad g_2(x)=k_2\begin{bmatrix}0\\0\\0\\0\\0\\0\\\frac{p_2}{m}\\-\frac{ma\cdot p_2}{J_y}\end{bmatrix}\quad g_1(x)=k_2\begin{bmatrix}0\\0\\0\\0\\\frac{p_3}{m}\\-\frac{mb\cdot p_3}{J_x}\\0\\0\end{bmatrix}\quad g_2(x)=k_2\begin{bmatrix}0\\0\\0\\0\\0\\0\\\frac{p_4}{m}\\\frac{mb\cdot p_4}{J_y}\end{bmatrix} \tag{11}$$

The disturbances caused by the residual static and dynamic imbalances are,

$$\begin{aligned}&\Delta(1)=\Delta(3)=\Delta(5)=\Delta(7)=0\\&\Delta(2)=-\overline{g}\cdot\Omega^2\cdot\sin(\Omega t+\alpha_s)\\&\Delta(4)=\overline{h}\cdot\Omega^2\cdot\sin(\Omega t+\alpha_d)\\&\Delta(6)=\overline{g}\cdot\Omega^2\cdot\cos(\Omega t+\alpha_s)\\&\Delta(8)=\overline{i}\cdot\Omega^2\cdot\cos(\Omega t+\alpha_d)\\&\overline{g}=m_sR/m\overline{h}=\overline{i}=2m_dRd/J_R\end{aligned}\tag{12}$$

R is radius and h is the height of the rotor. Eq. (13) are the output functions for the selected outputs.

$$\begin{cases}h_1(x)=x_{ma}=(x_1+L\cdot x_3)/2\\h_2(x)=x_{mb}=(x_1-L\cdot x_3)/2\\h_3(x)=y_{ma}=(x_5-L\cdot x_7)/2\\h_4(x)=y_{mb}=(x_5+L\cdot x_7)/2\end{cases}\tag{13}$$

3. Nonlinear observer design

The problem of state estimation is important for controller design of the nonlinear system (5). For system (5), it is obvious that $f(x^0,u^0)|_{x=0,u=0}=0$. It is supposed that its states in the neighborhood of $x^0=0$ can be estimated, and then the nonlinear state feedback linearization controller which based on the estimate values of the states could be applied to stabilize the unstable system. So an observer with exponential or asymptotic convergence characteristic is needed for the state estimation. A nonlinear Luenberger observer will be developed in this section [15,16].

The MSFW dynamics Eq. (5) has vector relative degrees defined by the *Lie derivative* $\mathbf{r}=[2222]$, and $r_1+r_2+r_3+r_4=8$. So a reversible coordinate mapping and a nonsingular *Jacobian* matrix would be defined as follows.

$$z=\Phi(x)=\begin{bmatrix}h_1(x) & L_fh_1(x) & \cdots & h_4(x) & L_fh_4(x)\end{bmatrix}^T\mathrm{Q}(x)=d\Phi/dx\tag{14}$$

$$x=\Phi^{-1}(z)\tag{15}$$

where $L_fh_i(x)$ is the standard *Lie derivative* of the $h_i(x)$ along the vector field $f(x)$. The system (5) can be transferred to a new form using the coordinate transformation (14) with matrix (17) and (18).

$$\begin{aligned}&\dot{z}=Az+BL(\Phi^{-1}(z))\\&y=Cz\end{aligned}\tag{16}$$

where A, B, C are the *Brunowsky* matrixes of MIMO linear state space model.

$$H(x)=\begin{bmatrix}L_{g_1}L_fh_1 & L_{g_2}L_fh_1 & \cdots & L_{g_4}L_fh_1\\L_{g_1}L_fh_2 & L_{g_2}L_fh_2 & \cdots & L_{g_4}L_fh_2\\\vdots & \vdots & \vdots & \vdots\\L_{g_1}L_fh_4 & L_{g_2}L_fh_4 & \cdots & L_{g_4}L_fh_4\end{bmatrix}_{4\times4}$$

$$=k_2\begin{bmatrix}(\frac{1}{M_{11}}+\frac{ma^2}{M_{22}})p_10(\frac{1}{M_{11}}-\frac{ma\cdot mb}{M_{22}})p_30\\(\frac{1}{M_{11}}-\frac{ma\cdot mb}{M_{22}})p_10(\frac{1}{M_{11}}+\frac{mb^2}{M_{22}})p_30\\0(\frac{1}{M_{33}}+\frac{ma^2}{M_{44}})p_20(\frac{1}{M_{33}}-\frac{ma\cdot mb}{M_{44}})p_4\\0(\frac{1}{M_{33}}-\frac{ma\cdot mb}{M_{44}})p_20(\frac{1}{M_{33}}+\frac{mb^2}{M_{44}})p_4\end{bmatrix}_{4\times4}\tag{17}$$

$$L(x)=\begin{bmatrix}L_f{}^2h_1(x)\\L_f{}^2h_2(x)\\L_f{}^2h_3(x)\\L_f{}^2h_4(x)\end{bmatrix}=\begin{bmatrix}f_2+ma\cdot f_4\\f_6-mb\cdot f_8\\f_2-ma\cdot f_4\\f_6+mb\cdot f_8\end{bmatrix}\tag{18}$$

The observer of system (5) could be developed based on the transformed system (16), which is obtained by the nonlinear coordinate transformation (14).

It is supposed that, the constructed Luenberger observer of the transformed system (16) has the form as following,

$$\dot{\hat{z}}=A\hat{z}+BL(\Phi^{-1}(\hat{z}))+K(y-C\hat{z})\tag{19}$$

If the following four conditions are satisfied,

(a) The system (5) is observable in R^8, and the transformation $z=\Phi(x)$is uniformly *Lipschitz* together with its inverse $x=\Phi^{-1}(z)$in R^8, with constant γ_Φ and $\gamma_{\Phi^{-1}}$, respectively.
(b) $H(\Phi^{-1})$ and $L(\Phi^{-1})$are uniformly *Lipschitz*, with constant $\gamma_{\overline{H}}$ and $\gamma_{\overline{L}}$, respectively.
(c) A constant $\mu_M>0$ exists such that $|\mu(t)|\le\mu_M$.
(d) For a given vector $K\in R^n$, a symmetric positive definite matrix $P\in R^{n\times n}$ exists that satisfies the following H_∞ *Riccat-liki* inequality.

$$(A-KC)P+P(A-KC)^T+BB^T+2\alpha P+\gamma^2P^2\le0\tag{20}$$

where $\gamma^2=\gamma_{\overline{L}}{}^2+u_M{}^2\cdot\gamma_{\overline{H}}{}^2$,

Let$K=\varepsilon^2PC^T$, and solve the standard *Riccati-like* inequality (20), the obtained matrix K will guarantee the convergence of the constructed nonlinear Luenberger observer (19).

From Eq. (19), the nonlinear observer of the original system (5) is,

$$\dot{\hat{x}}=f(\hat{x})+g(\hat{x})u(t)+Q^{-1}(\hat{x})K(y(t)-h(\hat{x}))\tag{21}$$

It is easily to verify that the HMBs system (5) satisfies the conditions (a)–(d). So the designed Luenberger observer (21) is exponential convergence, and then the states of the HMBs system could be obtained for the controller design.

4. Exact linearization and controller design

As the linear control theory is relatively complete, it is an effective method using the linear control theory to settle the nonlinear control problems. Different with linearization which uses the Taylor expansion and ignores the higher order components of the dynamic model, the exact linearization uses the coordinate transformation linearization and state-feedback linearization to transfer a nonlinear model to a linear one, and no high order part is ignored. The controller of the MSFW which uses the exact linearization technique is designed in this paper. [17,18].

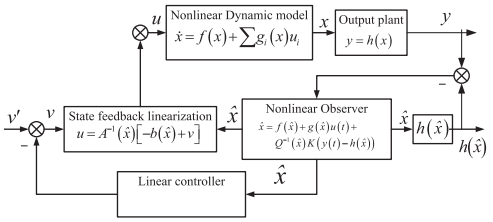

Fig. 7. The controller applied to the MSFW.

As shown in Fig. 7, it is the sketch of the designed controller applied to the MSFW.

4.1. Coordinate transformation linearization

The system dynamic equation can be transformed to a one with canonical form using the coordinate transformation linearization. It is obvious that the dynamic Eq. (5) is a standard dynamic model with canonical form already. So the nonlinear system (5) could be transferred to linear one using the state-feedback linearization only.

4.2. State-feedback linearization

It has been obtained that system (5) has the vector relative degree $\boldsymbol{r}=\{2\ 2\ 2\ 2\}$ at x^0, and $r=r_1+r_2+r_3+r_4=8$. So the system (5) can be linearized using the state feedback. The coordinate transformation is defined as following,

$$\begin{bmatrix}\xi_1 & \xi_2 & \cdots & \xi_8\end{bmatrix}^T=\phi(x)$$
$$=\begin{bmatrix}h_1(x) & L_fh_1(x) & \cdots & h_4(x) & L_fh_4(x)\end{bmatrix}^T \tag{22}$$

The feedback functions $A(x)$ and $b(x)$ are defined as following,

$$A(x)=\begin{bmatrix}L_{g_1}L_f^{r_1-1}h_1(x) & \cdots & L_{g_4}L_f^{r_1-1}h_1(x)\\ \vdots & & \vdots\\ L_{g_1}L_f^{r_4-1}h_4(x) & \cdots & L_{g_4}L_f^{r_4-1}h_4(x)\end{bmatrix} \tag{23}$$

$$b(x)=\begin{bmatrix}L_f^2h_1(x)\\ L_f^2h_2(x)\\ L_f^2h_3(x)\\ L_f^2h_4(x)\end{bmatrix}=$$
$$\begin{bmatrix}\{k_1\cdot[p_1^2\cdot(x_1+ma\cdot x_3)+p_3^2\cdot(x_1-mb\cdot x_3)]\}/M_{11}\\ \{k_1\cdot[ma\cdot p_1^2\cdot(x_1+ma\cdot x_3)-mb\cdot p_3^2\cdot(x_1-mb\cdot x_3)]\}/M_{22}\\ \quad+\left\{\bar{a}\sin(2\Omega t)\Omega\cdot x_4+\left[\bar{b}+\bar{c}\sin^2(\Omega t)\right]\Omega\cdot x_8\right\}\\ \{k_1\cdot[p_2^2\cdot(x_5-ma\cdot x_7)+p_4^2\cdot(x_5+mb\cdot x_7)]\}/M_{33}\\ \{k_1\cdot[-ma\cdot p_2^2\cdot(x_5-ma\cdot x_7)+mb\cdot p_4^2\cdot(x_5+mb\cdot x_7)]\}/M_{44}\\ \quad+\left\{\left[\bar{d}+\bar{e}\cos^2(\Omega t)\right]\Omega\cdot x_4+\bar{f}\sin(2\Omega t)\Omega\cdot x_8\right\}\end{bmatrix} \tag{24}$$

The function $A(x)$ is nonsingular in the neighborhood of $x^0=0$. If apply the state feedback (25) to the nonlinear system (5),

$$u=A^{-1}(x)\left[-b(x)+v\right] \tag{25}$$

The MIMO nonlinear system (5) could be transformed to a linear one in the form of,

$$\begin{cases}\begin{bmatrix}\dot{\xi}_1\\ \dot{\xi}_2\end{bmatrix}=\begin{bmatrix}0 & 1\\ 0 & 0\end{bmatrix}\begin{bmatrix}\xi_1\\ \xi_2\end{bmatrix}+\begin{bmatrix}0\\ 1\end{bmatrix}v_1+\Delta_1'\\ y_1=\xi_1\end{cases}$$

$$\begin{cases}\begin{bmatrix}\dot{\xi}_3\\ \dot{\xi}_4\end{bmatrix}=\begin{bmatrix}0 & 1\\ 0 & 0\end{bmatrix}\begin{bmatrix}\xi_3\\ \xi_4\end{bmatrix}+\begin{bmatrix}0\\ 1\end{bmatrix}v_2+\Delta_2'\\ y_2=\xi_3\end{cases}$$

Table 1
Parameters of the simulation MSFW system.

Symbol	Value	Symbol	Value
J_z	0.0286 kgm^2	m_s	40 mg
g	0.2 mm	m_d	15 mg
m	4.2 kg	α_s	0
H_c	780,000	α_d	π
u_0	$4\pi\times10^{-7}$	R	400 mm
u_r	1.05	d	70 mm
Ke	1.05	N	150
ma,mb	15 mm	L	25 mm
k_m	1.3		

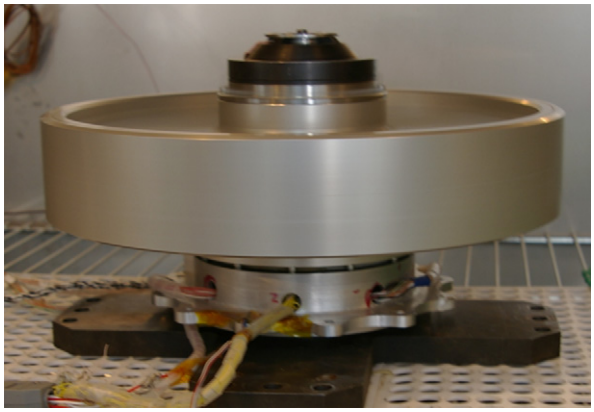

Fig. 8. The MSFW system which adopted the PM biased HMBs.

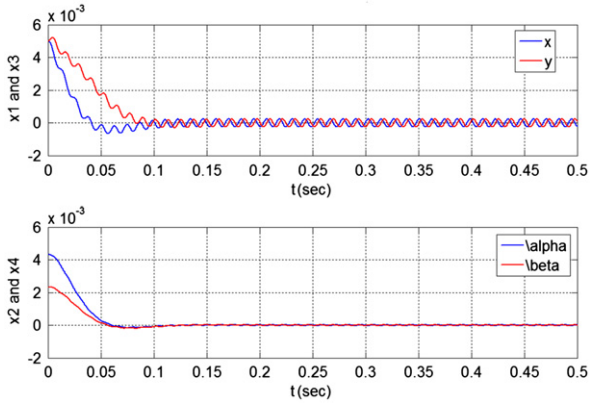

Fig. 9. The state variables of the MSFW with the spin rate of 5000 rpm.

$$\begin{cases} \begin{bmatrix} \dot{\xi}_5 \\ \dot{\xi}_6 \end{bmatrix} = \begin{bmatrix} 0 & 1 \\ 0 & 0 \end{bmatrix} \begin{bmatrix} z_5 \\ z_6 \end{bmatrix} + \begin{bmatrix} 0 \\ 1 \end{bmatrix} v_3 + \Delta_3' \\ y_3 = \xi_5 \end{cases}$$

$$\begin{cases} \begin{bmatrix} \dot{\xi}_7 \\ \dot{\xi}_8 \end{bmatrix} = \begin{bmatrix} 0 & 1 \\ 0 & 0 \end{bmatrix} \begin{bmatrix} \xi_7 \\ \xi_8 \end{bmatrix} + \begin{bmatrix} 0 \\ 1 \end{bmatrix} v_4 + \Delta_4' \\ y_4 = \xi_7 \end{cases} \quad (26)$$

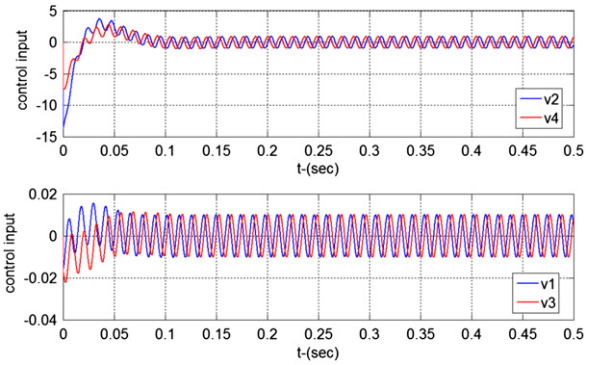

Fig. 10. The inputs applied to the linearized system with the spin rate of 5000 rpm of the MSFW.

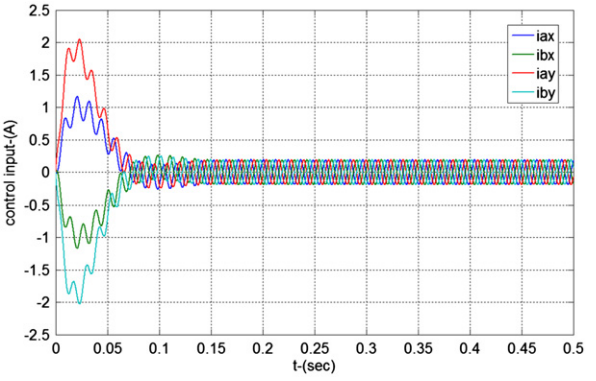

Fig. 11. The actual inputs applied to the nonlinear system with the spin rate of 5000 rpm of the MSFW.

4.3. Controller design

The exactly linearized dynamic model of MSFW system (26) consists of four decoupled SISO linear sub-systems. Almost all of linear controllers widely used can be applied to the control of every sub-system Take the simple state-feedback controller for example, the poles of the four sub-systems are assigned at $-0.8660 \pm 0.5000i$. The inputs applied on the linearized system (26) v can be regulated by the linear state-feedback controller, and then, the real inputs applied on the nonlinear system u can be calculated using (25) in the end.

5. Simulations and Experiments

5.1. Simulations

Parameters of the simulation MSFW are provided in Table 1. It is a prototype for the high-precision earth observation satellite. Fig. 8 is the photo of the simulated MSFW.

The initial state of the MSFW system is selected as $x_0=[5e^{-6}, 4.3e^{-3}, 5e^{-6}, 2.3e^{-3}, 0, 0, 0, 0]$, so the initial outputs of the rotor in *OXYZ* are (70 um, $^{-}$30 um), ($^{-}$60 um, 40 um). The spin rate of the rotor is 5000 rpm.

Fig. 9 is the simulation results of the state variables. Fig. 10 is the calculated inputs applied to the linearized system (26), and Fig. 11 is the real inputs applied to the nonlinear system (5). The outputs of the nonlinear system are described in details in Fig. 12.

It is obvious that, the designed controller can guarantee the stable suspension of the rotor at the simulated rotational speed. And the disturbances caused by the imbalances of the rotor could be depressed. Compared with the classical PID with cross feedback control strategy [19] usually used in the control of MSFW, it can be regarded that, the cross feedback has been taken into account in the state-feedback linearization and can realize the decoupling between coupled DOFs. The compared PID with cross feedback controller used in this paper is,

$$\begin{cases} i_{ax} = k_p x_{ma} + k_i \int x_{ma} dt + k_d \dot{x}_{ma} + k_c \Omega \cdot F(\beta) \\ i_{bx} = k_p x_{mb} + k_i \int x_{mb} dt + k_d \dot{x}_{mb} - k_c \Omega \cdot F(\beta) \\ i_{ay} = k_p y_{ma} + k_i \int y_{ma} dt + k_d \dot{y}_{ma} - k_c \Omega \cdot F(\alpha) \\ i_{by} = k_p y_{mb} + k_i \int y_{mb} dt + k_d \dot{y}_{mb} + k_c \Omega \cdot F(\alpha) \end{cases} \quad (27)$$

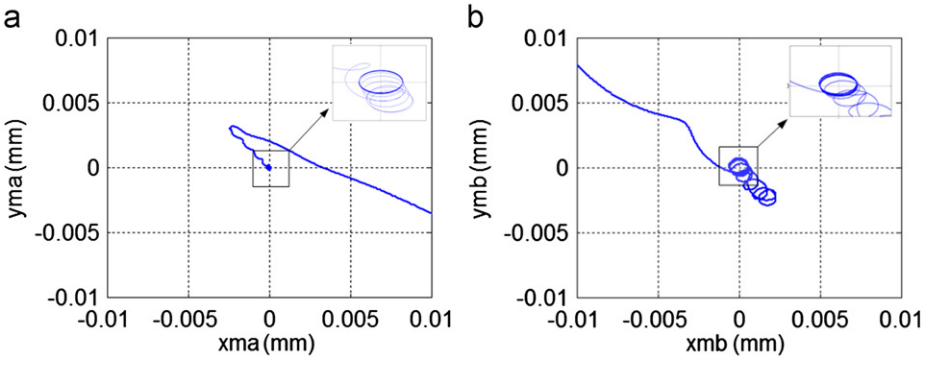

Fig. 12. The outputs of the nonlinear system with the spin rate of 5000 rpm of the MSFW.

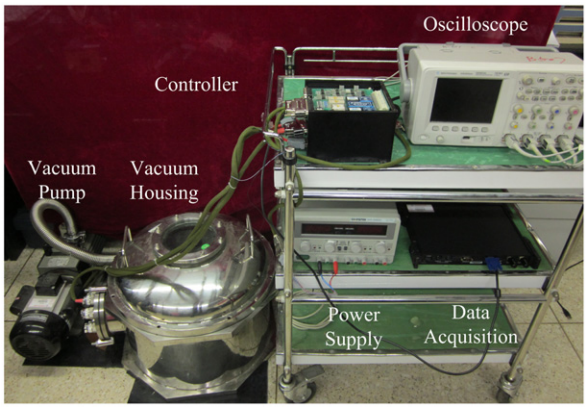

Fig. 13. The experiment system of the MSFW.

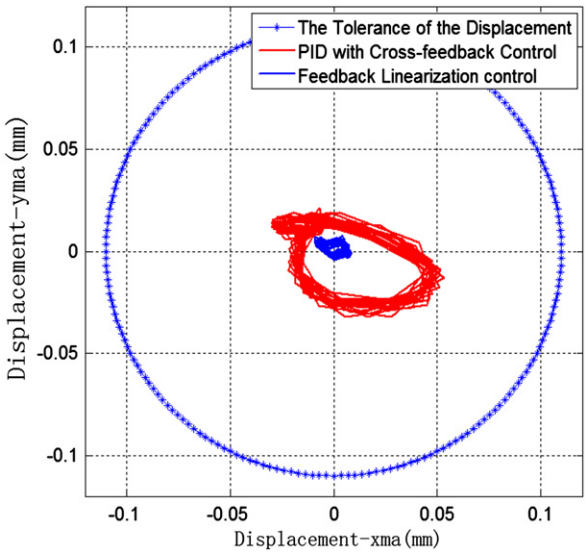

Fig. 14. The locus of the rotor when it is dominated by different control strategies in 5000 rpm.

This controller is designed based on the linear model realized by the Taylor expansion method. The coupling in different DOFs and higher order items of the magnetic forces are ignored in such linearization. The $k_c\Omega \cdot F(\beta)$ and $k_c\Omega \cdot F(\alpha)$ are the additional cross feedback items added into the outputs of the PID controller to depress the precession and nutation of the rotor caused by the gyro-effect of the rotating rotor. The function $F(\cdot)$ is the filter applied on the states of α and β to extract the precession and nutation motions of the rotor. The proportion, integration and differential coefficients of the PID controller are [3200 80 350], the dominant poles of the system are $-40 \pm 40i$. The coefficient k_c varies according to the rotating speed.

5.2. Experiments

As shown in Fig. 13, it is the experiment system of the MSFW. The system consists of controller, MSFW, data acquisition system, oscilloscope, vacuum housing and vacuum pump. The MSFW is operating in vacuum housing realized by the pump (<5 Pa) to eliminate the impact caused by the windage. The displacements and currents in the coils of the MSFW are monitored by the oscilloscope and recorded by the data acquisition system when the MSFW is rotating.

As shown in Fig. 14, it is the experiment results when the designed controller and the PID with Cross feedback controller are applying to the MSFW. The circle is the tolerance of the displacement of the rotor restricted by the back-up bearing. The radius of the circle is 0.11 mm. It is obviously that the outer locus is not symmetry with the origin of the center and greater than the inner one. Using the proposed feedback linearization controller, the displacements of the rotor are depressed greatly. The reduction of the displacement is benefit for the precision of the angular moment direction of the rotor, which determines the direction precision of the output torque produced by the MSFW.

Fig. 14 is currents i_{ax} and i_{ay} in the ax and ay coils when the rotor is spinning in 5000 rpm. The pk–pk of the currents

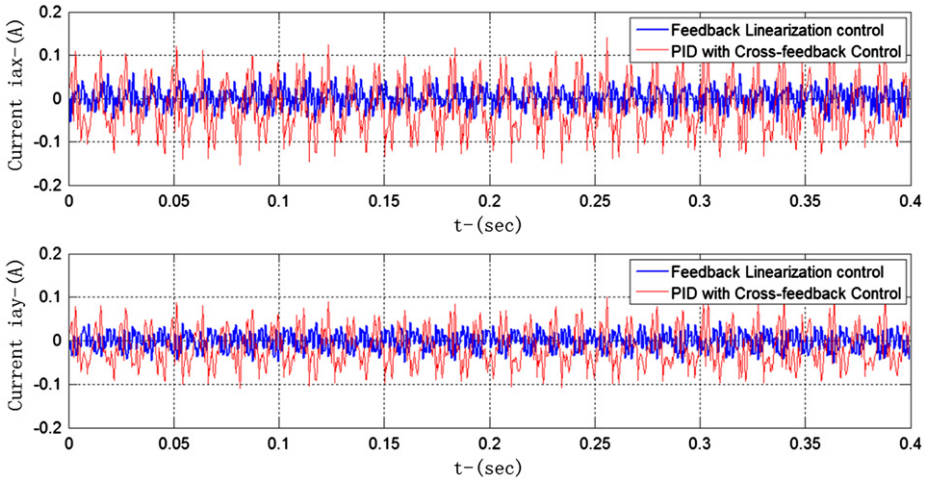

Fig. 15. The current i_{ax} and i_{ay} when the rotor is dominated by different control strategies in 5000 rpm.

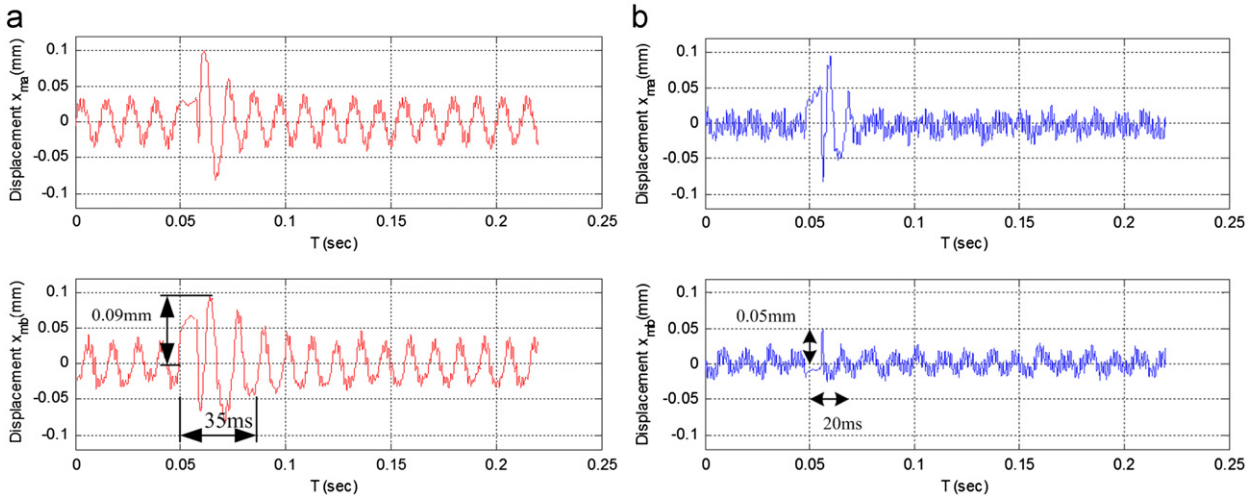

Fig. 16. The evaluation of the decoupling ability of the two controllers. (a) Adopted the PID with cross feedback controller, (b) adopted the feedback linearization controller.

are less than 0.1 A using the Feedback linearization control designed in this paper. The pk–pk is more than 0.2 A using the PID with Cross feedback control strategy Fig. 15.

In order to evaluate the decoupling ability of the two controllers, an impulse disturbance is injected into one DOF (x_{ma}) of the operating MSFW, the displacements of the rotor in the other DOF (x_{mb}) are monitored and recorded. The experiment shows that when the MSFW is dominated by the proposed controller, the regulating time and the overshoot of the displacement in x_{mb} are much less when the PID with cross feedback controller is used. As shown in Fig. 16, the regulating time is reduced from 35 ms to 20 ms, the overshoot is reduced from 0.09 mm to 0.05 mm.

6. Conclusion

In this paper, the dynamic model of the MSFW whose rotor is suspended by the HMBs has been obtained using the rotor dynamics and the magnetic forces expressions of the HMBs. The nonlinear dynamic has been exactly transformed to a linear state space model via state-feedback linearization. And then a linear controller based on the linearized model is designed to stabilize the rotor of the MSFW. Compare with the PID with Cross feedback controller, the benefits such as limited displacements, lower tuning currents, better decoupling ability are ensured by the simulations and experiments when the MSFW is regulated by the proposed controller.

References

[1] G. Schweitzer, E.H. Maslen, Magnetic Bearings: Theory, Design, and Application to Rotating Machiner, Springer Verlag, New York, 2009.
[2] J.C. Fang, J.J. Sun, H. Liu, et al., A novel 3-DOF axial Hybrid Magnetic bearing. magnetics, IEEE Trans. Magn. 46 (12) (2010) 4034–4045.
[3] J.Y. Hung, N.G. Albritton, F. Xia, Nonlinear control of a magnetic bearing system, Mechatronics 13 (6) (2003) 621–637.
[4] K.R. Rajagopal, K.K. Sivadasan, Low-stiction magnetic bearing for satellite application, J. Appl. Phys. 91 (10) (2002) 6994–6996.
[5] Aerospace flywheel technology development for IPACS applications, NASA Report, TM-2001-211093, 2001.
[6] J. Seddon, A. Pechev, 3Dwheel: 3-axis low noise, high-bandwidth attitude actuation from a single momentum wheel using magnetic bearings, Proceedings of 23rd Annual AIAA/USU Conference on Small Satellite, 2009;.
[7] M. Chen, C.R. Knospe, Feedback linearization of active magnetic bearings: current-mode implementation, IEEE/ASME Trans. Mechatron. 10 (6) (2005) 632–639.
[8] R.D. Smith, W.F. Weldon, Nonlinear control of a rigid rotor magnetic bearing system: Modeling and simulation with full state feedback, IEEE Trans. Magn. 31 (2) (1995) 973–980.
[9] M.J. Jang, C.L. Chen, Y.M. Tsao, Sliding mode control for active magnetic bearing system with flexible rotor, J. Franklin Inst. 342 (4) (2005) 401–419.
[10] A.E. Rundell, S.V. Drakunov, R.A. DeCarlo, A sliding mode observer and controller for stabilization of rotational motion of a vertical shaft magnetic bearing, IEEE Trans. Control Syst. Technol. 4 (5) (1996) 1063–6536.
[11] Z.J. Yang, M. Tateishi, Adaptive robust nonlinear control of a magnetic levitation system, Automatica 37 (7) (2001) 1125–1131.
[12] L. Gentili, L. Marconi, Robust nonlinear disturbance suppression of a magnetic levitation system, Automatica 39 (4) (2003) 735–742.
[13] S. Sivrioglu, K. Nonami, Adaptive output backstep-ping control of a flywheel zero-biased AMB system with parameter uncertainty, Proceedings of the 42nd IEEE Conference on Decision and Control, 2003, pp. 3942–3947.
[14] T. Dever, G. Brown, K. Duffy, et al., Modeling and development of a magnetic bearing controller for a high speed flywheel system, Proceeding of 2nd International Energy Conversion Engineering Conference, 2004.
[15] G. Ciccarella, M.M. Dalla, A. Germani, A. Luenber-ger-like, Observer for nonlinear systems, Int. J. Control 57 (3) (1993) 537–556.
[16] M.D. Mora, A. Germani, C. Manes, A State Observer for Nonlinear Dynamic Systems, Proc. 2nd Word Congress of Nonlinear Analysis, 1997, 4485-4496.
[17] A. Isidori, Nonlinear Control Systems, 2nd edn, Springer Verlag, New York, 1995.
[18] J.D. Lindlau, C.R. Knospe, Feedback linearization of an active magnetic bearing with voltage control, IEEE Trans. Control Syst. Technol. 10 (1) (2005) 21–31.
[19] X.H. Tian, J.C. Fang, G. Liu, Analysis and testing of MSFW with gain-scheduled proportional cross feed-back control, Proceeding of the 8th International Symposium on Magnetic Suspension Technology, 2005, pp.187-191.